

Measurement-induced entanglement of two transmon qubits by a single photon

Christoph Ohm and Fabian Hassler

*JARA Institute for Quantum Information, RWTH Aachen University, 52056 Aachen, Germany**

(Dated: August 2015)

On-demand creation of entanglement between distant qubits is desirable for quantum communication devices but so far not available for superconducting qubits. We propose an entanglement scheme that allows for single-shot deterministic entanglement creation by detecting a single photon passing through a Mach-Zehnder interferometer with one transmon qubit in each arm. The entanglement production essentially relies on the fact that superconducting microwave structures allow to achieve strong coupling between the qubit and the photon. By detecting the photon via a photon counter, a parity measurement is implemented and the wave function of the two qubits is projected onto a maximally entangled state. Moreover, due to the indivisible nature of single photons, our scheme promises full security for entanglement-based quantum key distribution.

PACS numbers: 03.67.Bg 42.50.Dv 42.50.Pq 85.25.-j

Entanglement is one of the most characteristic features distinguishing quantum mechanics from classical mechanics [1] and its paradoxical predictions have challenged generations of physicists, see e.g. [2]. Quantum information theory aims to exploit entanglement as a resource for protocols guaranteeing secure quantum communication over macroscopic distances, namely quantum teleportation [3] and quantum key distribution [4].

The pioneering works of Refs. [5] and [6] have shown that entanglement can not only be transferred via direct interactions, but also by performing a measurement such that the wave function is projected onto an entangled state. This method, known as entanglement swapping, is based on the indistinguishability of the quantum states compatible with the measurement outcome and constitutes one of the key ingredients used for quantum repeaters [7]. Moreover, the genesis of entanglement by performing a measurement has been first proposed for atoms in a quantum optical framework [8, 9]. Since then, measurement-induced entanglement of remote quantum systems has been experimentally demonstrated for diverse atomic setups [10–12] as well as for solid state qubit devices such as nitrogen vacancy centers [13] and superconducting qubits [14].

To our knowledge, none of these schemes is capable of generating on-demand entanglement in a fast and secure fashion with single-shot efficiency as desired for quantum communication protocols. The main obstacle is that the light-matter interaction is weak in the range of optical frequencies. To overcome this problem most quantum optical entangling-schemes exploit the photon polarization degree of freedom, whereas other proposals suggest to use more challenging concepts such as NOON-states [15]. Furthermore, since the emission of optical photons is an undirected process, all these settings suffer from a low photon collection efficiency.

In contrast, in circuit quantum electrodynamics (cQED), which deals with superconducting qubits and their interaction to microwave radiation, it has been

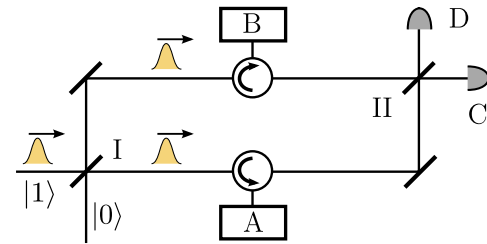


FIG. 1. Mach-Zehnder interferometer made of two 50:50 beamsplitters (I and II). Each arm of the interferometer is coupled to a microwave resonator (A and B) which in turn is dispersively coupled to a transmon qubit. A single-photon wave-packet that is sent into the MZI causes a click in one of the two detectors at the outputs. The projective measurement due to the photon counters implements a parity measurement on the transmon qubits. As a result, irrespective of which photon detector (C or D) clicks, the wave function is projected on a maximally entangled two-qubit state.

possible to reach the strong coupling regime in which the light-matter coupling is stronger than typically induced dissipation scales [16]. Even though microwave photons are typically unpolarized, present cQED-implementations accomplished measurement-induced entanglement of superconducting qubits with sufficient efficiency via coherent states, either with the qubits placed inside a single cavity [17] or in separate resonators [14]. Due to the lack of erasure of the which-path information, these protocols only offer a maximal efficiency of 50%. More recently, it has been understood that employing additionally a non-linear element maximum efficiency is achievable [18, 19]. The quantum mechanical state projection is caused in all these cases by a weak continuous measurement [20, 21]. Because of that, entanglement emerges only rather slowly with the wave function gradually collapsing in time. Furthermore, the usage of semiclassical radiation, involving signals with many photons, allows for the generation of multi-partite entanglement [22, 23]. In turn, the possibility of such multi-partite en-

tanglement bears the risk of eavesdropping and therefore renders the Ekert protocol for quantum key distribution insecure [4].

Here, we propose a novel scheme for entangling superconducting transmon qubits over a distance by using a strong projective measurement of a single microwave photon. The photon propagates through a Mach-Zehnder interferometer (MZI) containing two transmon qubits to be entangled. Relying on the discreteness of photonic Fock states as well as the ability of cQED to access the strong coupling regime, our scheme prohibits eavesdropping during the entanglement generation as required for a secure key distribution. Within the last decade, cQED has become a mature field of quantum engineering technology promising integrated and scalable circuits suitable for quantum computation. In particular, the generation of single microwave photons in superconducting circuits [24] and moreover the controlled creation of entanglement between microwave photons and transmon qubits has been reported [25]. These promising attempts towards well-controlled microwave photonics encouraged us to suggest an entanglement protocol taking advantage of the high efficiencies in cQED combined with single-shot (projective) measurements.

The outline of the paper is as follows. First, we will explain the generation of entanglement by introducing the interferometric apparatus and discuss the procedure under ideal conditions. Subsequently, a more general analysis clarifies the conditions under which maximal entanglement is achievable. Specifically, we will discuss the case of entanglement generated by a Lorentzian-shaped single-photon wave-packet as well as the entanglement in case of non-identical cavities.

At the first beamsplitter, an incoming photon is split into two partial waves $|\psi_{\text{ph}}\rangle = (|1_A, 0_B\rangle + |0_A, 1_B\rangle)/\sqrt{2}$, each traversing one arm (A or B) of the interferometer. After having passed the second beamsplitter, the partial waves are recombined and the photon escaped into one of the two output channels C and D, see Fig. 1. If both partial waves acquire a relative phase difference of $\varphi = 0$ while passing the MZI, i.e., if both partial waves accumulate exactly the same phase in both arms A and B, the photon is transmitted into channel C with certainty. On the other hand, if the partial waves accumulate a relative phase difference of $\varphi = \pi$, the photon is transmitted into mode D. Due to this single-photon interference effect, the MZI distinguishes between certain qubit states: by placing two dispersively interacting transmon qubits A and B in each arm of the interferometer as shown in Fig. 1, each partial wave picks up an individual phase due to scattering from these distinct qubits. If the qubits are initialized in a state spanned by the subspace $|\uparrow_A, \uparrow_B\rangle, |\downarrow_A, \downarrow_B\rangle$, the scattering phases on are identical in both arms and the photon is transmitted into channel C. If on the other hand, the qubits are in a state spanned by $|\uparrow_A, \downarrow_B\rangle, |\downarrow_A, \uparrow_B\rangle$ and if the scattering induces a rela-

tive phase difference of $\varphi = \pi$, then the photon is transmitted only into channel D. Hence, the interference of the partial waves allows for a parity-selective transmission of the photon through the MZI, discriminating the states $|\uparrow_A, \uparrow_B\rangle, |\downarrow_A, \downarrow_B\rangle$ with even parity from the states $|\uparrow_A, \downarrow_B\rangle, |\downarrow_A, \uparrow_B\rangle$ with odd parity. As a consequence of this parity-selective single-photon interference, the MZI can be used to measure the qubit parity $P = \sigma_{z,A}\sigma_{z,B}$. Once the photon is registered in one of the detectors C or D, the wave function collapses onto a state with definite parity, $P = 1$ (even parity) or $P = -1$ (odd parity). Furthermore, such a parity measurement is useful for entanglement preparation like other solid-state implementations suggest [26–30], but here entanglement is accomplished with single-shot efficiency.

The protocol proceeds as follows: we initialize the qubits in the superposition $|+_A, +_B\rangle$ with $|+_j\rangle = (|\uparrow_j\rangle + |\downarrow_j\rangle)/\sqrt{2}$ for each qubit $j = A, B$. This state is—among other possibilities—a suitable choice and due to the dispersive interaction $\propto \sigma_{z,j}a_j^\dagger a_j$ each partial wave of the photon introduces state-dependent scattering phases φ_\uparrow and φ_\downarrow to the qubit: $(|\uparrow_j\rangle + |\downarrow_j\rangle)/\sqrt{2} \mapsto (e^{i\varphi_\uparrow}|\uparrow_j\rangle + e^{i\varphi_\downarrow}|\downarrow_j\rangle)/\sqrt{2}$ within each arm. Crucially, we demand the phase difference to be $\varphi_\downarrow - \varphi_\uparrow = \pi$ in order to make the MZI parity-discriminating. Note that such a large difference between the scattering phases can only be implemented within the strong coupling regime. After the photon is reflected off the cavities, it carries information about the qubit state as well as about the path it has taken. As this makes the states distinguishable we use the second beamsplitter (II) to erase the which-path information of the photon. In terms of the output Fock modes C and D the resulting state reads $(|\Phi^-\rangle|1_C, 0_D\rangle + |\Psi^-\rangle|0_C, 1_D\rangle)/\sqrt{2}$. Recasting the final state in terms of the Bell states

$$|\Phi^-\rangle = \frac{1}{\sqrt{2}}(|\uparrow_A, \uparrow_B\rangle - |\downarrow_A, \downarrow_B\rangle) \quad \text{with } P = 1, \quad (1a)$$

$$|\Psi^-\rangle = \frac{1}{\sqrt{2}}(|\uparrow_A, \downarrow_B\rangle - |\downarrow_A, \uparrow_B\rangle) \quad \text{with } P = -1, \quad (1b)$$

reveals the parity-selectivity of the MZI and shows furthermore that, due to the missing which-path information, the parity measurement is not able to distinguish in which arm the photon has scattered. Hence, the state projection leaves the qubits in an entangled state no matter in which detector the photon is registered. Taking the measurement outcome as starting point, every other entangled two-qubit state can be prepared by means of single qubit gates. In this sense, the protocol accomplishes deterministic entanglement with single-shot efficiency.

In the following, we will look at this scheme on a more formal level that allows to discuss imperfections. The crucial part of the photon propagation is the scattering process with the cavities and the qubits inside of these. In order to describe the cavity-qubit subsystems, we assume for simplicity that each qubit j is coupled to a single

cavity mode with frequency ω_c . The qubit states are separated by an energy splitting $\hbar\Delta$ which is considered to be far detuned from the resonance frequencies of the cavities, $\omega_c \gg \Delta$. In this regime, the light-matter coupling gives rise to a qubit-state dependent renormalization of the cavity frequency—the dispersive shift $\chi\sigma_{z,j}$. Accordingly, each cavity-qubit subsystem is then described by the Hamiltonian

$$H_j = \hbar\omega_c a_j^\dagger a_j + \frac{\hbar\Delta}{2}\sigma_{z,j} + \hbar\chi\sigma_{z,j}a_j^\dagger a_j, \quad (2)$$

where a_j, a_j^\dagger are creation and annihilation operators of the cavity modes obeying the canonical commutation relations $[a_j, a_l^\dagger] = \delta_{jl}$. A photon $b_{\text{in},j}(k)$, incident to arm j of the MZI with wave number $k > 0$ and frequency $\omega_k = c|k|$, induces a qubit-state dependent phase shift after being scattered off the cavity. This process is completely characterized by the reflection coefficient

$$r(\omega_k; \sigma_{z,j}) = \frac{i(\omega_c + \chi\sigma_{z,j} - \omega_k) - \kappa/2}{i(\omega_c + \chi\sigma_{z,j} - \omega_k) + \kappa/2} \quad (3)$$

which relates incoming and outgoing modes of the MZI by $b_{\text{out},j} = r_j(\omega_k; \sigma_{z,j})b_{\text{in},j}$ [31]. In (3), κ denotes the spectral broadening of the cavities. Due to the occurrence of the $\sigma_{z,j}$ terms, the qubit states $|\uparrow_j\rangle$ and $|\downarrow_j\rangle$ accumulate the relative phase difference $\varphi = \arg[r(\omega_k; \sigma_z = 1)] - \arg[r(\omega_k; \sigma_z = -1)]$ while the photon passes the interferometer. To achieve maximal entanglement between the qubits, it is crucial to generate a relative π phase shift, i.e., we would like to adjust the parameters of the device such that

$$\pi = \arg[r(\omega_k; \sigma_{z,j} = 1)] - \arg[r(\omega_k; \sigma_{z,j} = -1)] \quad (4)$$

for both qubits A and B. Condition (4) can be fulfilled by tuning the photon frequency to be

$$\Omega = \omega_c \pm (\chi^2 - \kappa^2/4)^{1/2}. \quad (5)$$

Note that these frequency sweet spots do only exist in the strong coupling regime where $2\chi \geq \kappa$. For convenience we will only consider one solution in (5) and omit the other one; this particular choice will be of no importance for the following analysis as long as we consistently stick to it. Recombining the two arms of the interferometer, the second beamsplitter acts as linear transformation upon the outgoing modes A, B and defines the output modes C, D via

$$\begin{pmatrix} c_{\text{out}} \\ d_{\text{out}} \end{pmatrix} = \frac{1}{\sqrt{2}} \begin{pmatrix} 1 & e^{i\theta} \\ -1 & e^{i\theta} \end{pmatrix} \begin{pmatrix} b_{\text{out},A} \\ b_{\text{out},B} \end{pmatrix}. \quad (6)$$

The phase shift $\theta = k(\ell_B - \ell_A)$ keeps track of the individual path lengths ℓ_j the photon has to take in each arm of the interferometer. As we will see later, this parameter turns out to be useful to prevent disturbing interferences

that negatively affect the degree of entanglement. Finally, after passing II, the photon is absorbed by one of the detectors C and D thereby projecting the transmon qubits onto an entangled state.

However, several erroneous mechanisms may spoil the production of full entanglement and lead to limitations of our scheme: the shape of the photon wave-packet, the fine tuning of cavity parameters, dissipative photon propagation due to leaky cavities or imperfect circulators, and efficiency of microwave photon counters. Since only the first two points one are inherent to the entanglement protocol, we want to focus our discussion on these intrinsic aspects. The latter points arise because of (extrinsic) technological limitations: If the circuit elements or the circulators are leaky, there is a finite probability for the photon to transmit into unwanted channels. This causes the reflection amplitude to have modulus less than one which lowers the photon count efficiency as well as the entanglement of the obtained state. The most serious experimental problem is the detection of single microwave photons. Although technically already possible, it remains a challenging task to build microwave photon counters working at high efficiency, see [32–34]. However, given the rapid progress in the field of cQED in the last decade, we are confident that the technological challenges will be addressed in the near future.

For a non-ideal setup, the photon measurement yields—depending on the outcome—projected states $|\Psi^m\rangle$ and $|\Phi^m\rangle$ that generally deviate from a Bell state. In order to quantify the degree of entanglement, we determine the fidelity of the outcome after the measurement and the wanted Bell state; the fidelity is a measure of distance between states in Hilbert space and is defined as $F[\psi, \phi] = |\langle\psi|\phi\rangle|^2$ for two arbitrary pure states $|\psi\rangle$ and $|\phi\rangle$, see [35]. Specifically, we are interested in the fidelities $F[\Phi^m, \Phi^-]$ or $F[\Psi^m, \Psi^-]$, depending on the measurement outcome. If these quantities take the value one, the projected state is the sought-after Bell state. In the following, we demonstrate how intrinsic errors affect the entanglement production and compute how the fidelity is affected by a single-photon wave-packet with Lorentzian wave profile as well as for non-identical cavities.

Generally, a single traveling photon is emitted as a wave-packet, i.e., a superposition of various frequencies. In other words, it becomes impossible to fulfill (4) for a generic photon state. For concreteness, we assume that the single microwave photon is produced from the controlled decay of a microwave resonator which means that the envelope function is a Lorentzian wave-packet

$$f(k) = \frac{(c\Gamma)^{1/2}}{i(\omega_k - \Omega) - \Gamma/2} \quad (7)$$

with spectral broadening Γ and the mean frequency tuned to Ω . Importantly, the relative weight factor η between qubit states $|\uparrow_j\rangle$ and $|\downarrow_j\rangle$, which is implied by

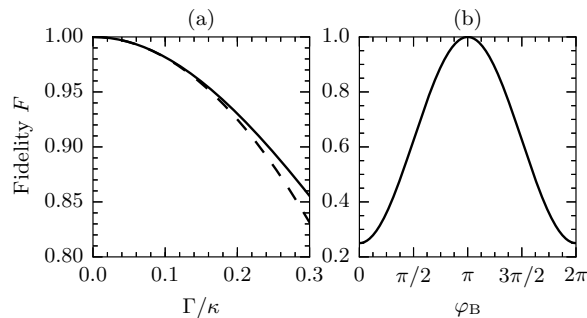


FIG. 2. Fidelities $F[\Psi^m, \Psi^-]$ of the protocol for the two two intrinsic error mechanisms as discussed in the main text. In (a), the fidelity $F[\Psi^m, \Psi^-]$ is shown as function of the spectral broadening in case a Lorentzian-shaped photon wave-packet passing the MZI (for $\chi = 2\kappa$). The solid line is obtained numerically whereas the dashed line corresponds to Eq. (8); both results agree in the regime $\Gamma \ll \kappa$. In (b), the fidelity (9) is shown as a function of the parameter φ_B , quantifying the detuning of cavity B, while assuming that cavity A is perfectly tuned. The ideal case corresponds to $\varphi_B = \pi$ with fidelity $F = 1$.

the dispersive interaction, can be represented as a coherent sum over all frequency components in the wave-packet, see also the Appendix. While the central frequency component of the photon wave-packet $\omega_k = \Omega$ reveals a relative phase factor of $e^{i\pi}$, all other frequency components induce relative phase factors deviating from this value. By averaging coherently over all these contributions the resulting weight factor η has modulus less than one, $|\eta| < 1$, and an average phase $\varphi = \arg(\eta) \neq \pi$ which generally differs from π . In particular, for the Lorentzian wave-packet the fidelity is a function of the photon spectral width Γ . Assuming $2\chi > \kappa$ [36], $\theta = 0$, and focussing to the limit $\Gamma/\kappa \ll 1$ we find the fidelity

$$F[\Phi^m, \Phi^-] \simeq 1 - 2[1 - (\kappa/2\chi)^2](\Gamma/\kappa)^2, \quad (8)$$

see Fig. 2 and the Appendix. Equation (8) holds if the photon has been registered in the detector C. For the reciprocal measurement outcome we find, due to parity-selective interference amplitudes, $F[\Psi^m, \Psi^-] = 1$ irrespective of the line width, see the Appendix for details. As Γ/κ approaches zero, the fidelity (8) becomes unity thereby achieving full, deterministic entanglement, i.e., for any measurement outcome.

Moreover, in a realistic setup the cavities will always be fabricated slightly differently. As a consequence, the frequency sweet spots of cavity A and B differ from each other, i.e., $\Omega_A \neq \Omega_B$. This implies that we can, at best, tune the (central) frequency of the photon to fulfill Eq. (4) on one side, say Ω_A . Then, according to (5) the dispersive interaction induces a relative weight factor $\eta_A = e^{i\pi}$ between states $|\uparrow_A\rangle$ and $|\downarrow_A\rangle$ of qubit A. Since the other cavity cannot fulfill (5) at the same time, it induces a distinct relative weight factor $\eta_B = e^{i\varphi_B} \neq -1$

where φ_B is a function of the parameters $\omega_{c,B}$, χ_B , and κ_B . By choosing the phase of the interferometer θ properly, φ_B remains the only parameter that cannot be controlled in situ, see the Appendix. Expressed as a function of φ_B , the fidelity reads

$$F[\Phi^m, \Phi^-] = F[\Psi^m, \Psi^-] = \frac{1}{8}[5 - 3\cos(\varphi_B)]. \quad (9)$$

When the parameters of both cavities coincide φ_B takes the value π and we recover the ideal case as indicated by a unit fidelity.

To be more specific, we want to discuss the case where cavities A and B only differ by their resonance frequency $\delta\omega = \omega_{c,B} - \omega_{c,A} \neq 0$ with all other parameters identical. Expanding φ_B in terms of the small parameter $\delta\omega/\kappa$ we find $\varphi_B \approx \pi + 4(1 - \kappa^2/4\chi^2)^{1/2} \delta\omega/\kappa$ for $\chi > \kappa/2$. Hence, the fidelity is

$$F[\Phi^m, \Phi^-] \simeq 1 - 3[1 - (\kappa/2\chi)^2](\delta\omega/\kappa)^2. \quad (10)$$

Equations (8) and (10) suggest to tune the cavities in both cases such that κ is sufficiently large as compared to the photon line width and the cavity detuning. However, since Eq. (5) sets an upper limit $\chi \geq \kappa/2$ for the magnitude of κ , the optimal implementation is a tradeoff between κ being larger than the photon line width and the cavity detuning, but still smaller than the dispersive shift.

In summary, we have proposed a novel method to entangle distant transmon qubits by single-shot photon measurements. Relying on the ability to access the strong coupling regime as well as the discrete nature of the Fock state microwave photons, our scheme represents a parity meter based upon strong projective measurements as opposed to previous approaches involving weak continuous measurements. We have analyzed the entanglement protocol under non-ideal conditions by demonstrating the sensitivity of the entanglement in terms of the fidelity for a photon, emitted with a finite line width, as well as for inaccurate parameter fine tuning of the cavities. Furthermore, we have argued that for an optimal implementation the magnitude of the cavity broadenings have to be on an intermediate scale limited from above by the light-matter coupling strength. Although the lack of high efficiency microwave photon counters remains a technological challenge for the entanglement protocol, we believe our method has potential applications for high-speed quantum communication protocols and rehabilitates a secure quantum key distribution for cQED implementations.

We acknowledge financial support from the Alexander von Humboldt Foundation.

APPENDIX

Transmission line coupling

An arm of the MZI is considered to be a one-dimensional superconducting transmission line guiding microwave photons from beamsplitter I to beamsplitter II. Accordingly, each arm ($j = A, B$) of the MZI hosts a one-dimensional continuum of modes

$$H_{\text{tl},j} = \int \frac{dk}{2\pi} \hbar\omega_k b_j^\dagger(k) b_j(k). \quad (11)$$

The mode operators $b_j^\dagger(k)$ and $b_j(k)$, obeying the commutation relations $[b_j(k), b_l^\dagger(k')] = 2\pi\delta_{jl}\delta(k-k')$, create and annihilate photon states from the vacuum in arm j of the MZI. The wave number k of a photon is related to its frequency ω_k by the linear dispersion relation $\omega_k = c|k|$. In our setup each transmission line (arm of the MZI) is intercepted by a microwave resonator enclosing a transmon qubit. For simplicity both cavities are characterized by a single mode described by operators a_j^\dagger and a_j . The transmon qubit inside a cavity is dispersively coupled to the cavity mode. Therefore we can describe each cavity-transmon subsystem by Eq. (2) of the main text. Photons inside the cavity can leak into the transmission line and vice versa. This process is described by the coupling Hamiltonian

$$H_{\text{cp},j} = \hbar\sqrt{c\kappa_j} \int \frac{dk}{2\pi} [b_j^\dagger(k)a_j + a_j^\dagger b_j(k)] \quad (12)$$

where κ_j characterizes the degree of hybridization between the cavity and its environment. Then, photons from the transmission line, which enter the cavity, interact with the qubit inside the cavity and are re-emitted into the transmission line. This scattering process is captured by the total Hamiltonian

$$H_{\text{tot},j} = H_j + H_{\text{tl},j} + H_{\text{cp},j}. \quad (13)$$

Far apart from the cavities for $|x| \rightarrow \infty$, photons in the transmission lines are considered to be freely propagating with respect to $H_{\text{tl},j}$. This suggests the definition of the time-dependent input and output fields

$$b_{\text{in},j}(x, t) = \int \frac{dk}{2\pi} e^{-i[\omega_k(t+T)-kx]} b_{\text{in},j}(k), \quad (14a)$$

$$b_{\text{out},j}(x, t) = \int \frac{dk}{2\pi} e^{-i[\omega_k(t-T)-kx]} b_{\text{out},j}(k), \quad (14b)$$

where the operators $b_{\text{in},j}(k) = b_j(k)|_{t=-T}$ and $b_{\text{out},j}(k) = b_j(-k)|_{t=T}$ generate asymptotically free scattering states for $T \rightarrow \infty$. For simplicity we will omit the space coordinate in the following and consider only the point $x = 0$ where the transmission line is connected to the cavity. As follows from standard input-output theory for cavities [31, 37], the input and output fields in Eqs. (14a)

and (14b) obey the boundary equation

$$b_{\text{out},j}(t) - b_{\text{in},j}(t) = \sqrt{c\kappa_j} a_j(t). \quad (15)$$

Here $a_j(t)$ is the time-dependent cavity operator which is subject to the Heisenberg equations of motion

$$\dot{b}_j(k) = -i\omega_k b_j(k) - i\sqrt{c\kappa_j} a_j, \quad (16a)$$

$$\dot{a}_j = -i(\omega_{c,j} + \chi\sigma_{z,j}) a_j - i\sqrt{c\kappa_j} \int \frac{dk}{2\pi} b_j(k), \quad (16b)$$

$$\dot{\sigma}_{z,j} = 0. \quad (16c)$$

The formal solution of Eq. (16a)

$$b_j(k; t) = e^{-i\omega_k(t+T)} b_{\text{in},j}(k) + \sqrt{c\kappa_j} \int_{-T}^t dt' e^{-i\omega_k(t-t')} a(t') \quad (17)$$

can be iterated into Eq. (16b). As a result, one obtains the quantum Langevin equation

$$\dot{a}_j = -i(\omega_{c,j} + \chi_j\sigma_{z,j}) a_j - \frac{\kappa_j}{2} a_j + \sqrt{c\kappa_j} b_{\text{in}}(t) \quad (18)$$

where the input field plays the role of an external driving. By using Eq. (15) and the quantum Langevin equation, one can derive the input-output relation

$$b_{\text{out},j}(k) = r_j(\omega_k; \sigma_{z,j}) b_{\text{in},j}(k) \quad (19)$$

where input and output fields are related to each other via the frequency-dependent reflection coefficient given in Eq. (3). Note that due to the lack of transmission into other channels than the reflection channel, the reflection coefficient is a complex number with modulus one, $|r_j| = 1$. Furthermore, the complex phase of $r_j(\omega_k; \sigma_{z,j})$ is the qubit state-dependent scattering phase that a photon acquires after being reflected from one of the two cavities.

Fidelities of the projected wave functions

In order to obtain a general expression for the fidelities, it has to be taken into account that photons usually are emitted as wave-packets. Therefore it is convenient to introduce wave-packet operators

$$B_j^\dagger = \int \frac{dk}{2\pi} f(k) b_j^\dagger(k) \quad (20)$$

that create single photons with a certain wave profile $f(k)$ from the vacuum state in arm j of the interferometer. To ensure that these wave-packets carry the intensity of one photon, the envelope function has to be normalized to one, $\int \frac{dk}{2\pi} |f(k)|^2 = 1$. Accordingly, the state of an incoming photon, which has been split by beamsplitter I, can be represented as

$$|\psi_{\text{ph}}\rangle = \frac{1}{\sqrt{2}} (B_A^\dagger + B_B^\dagger) |0\rangle. \quad (21)$$

After the photon has scattered with the qubits inside the MZI, the two modes $b_{\text{out,A}}$ and $b_{\text{out,B}}$ of arms A and B are converted into the output modes

$$c_{\text{out}} = \frac{1}{\sqrt{2}} (b_{\text{out,A}} + e^{i\theta} b_{\text{out,B}}), \quad (22)$$

$$d_{\text{out}} = \frac{1}{\sqrt{2}} (-b_{\text{out,A}} + e^{i\theta} b_{\text{out,B}}) \quad (23)$$

by the second beamsplitter (II) to erase the which-path information of the photon. The phase shift $\theta = k(\ell_B - \ell_A)$ arises due to the difference of the optical paths of the photon in the interferometer. Then, by detecting the photon in one of the output modes C or D, the total wave function $|\psi\rangle = |\psi_{\text{qb}}\rangle \otimes |\psi_{\text{ph}}\rangle$ is projected onto one of the states

$$|\Phi^{\text{m}}\rangle = \frac{c_{\text{out}}(t) |\psi\rangle}{\langle \psi | c_{\text{out}}^\dagger c_{\text{out}} | \psi \rangle^{\frac{1}{2}}}, \quad \text{or} \quad |\Psi^{\text{m}}\rangle = \frac{d_{\text{out}}(t) |\psi\rangle}{\langle \psi | d_{\text{out}}^\dagger d_{\text{out}} | \psi \rangle^{\frac{1}{2}}}.$$

In particular, the projected wave functions can be represented as

$$|\Phi^{\text{m}}\rangle = \frac{1}{\sqrt{N_\Phi}} \sum_{\sigma, \sigma'} (f_{\sigma, \text{A}} + f_{\sigma', \text{B}}) |\sigma_{\text{A}}, \sigma'_{\text{B}}\rangle, \quad (24\text{a})$$

$$|\Psi^{\text{m}}\rangle = \frac{1}{\sqrt{N_\Psi}} \sum_{\sigma, \sigma'} (f_{\sigma, \text{A}} - f_{\sigma', \text{B}}) |\sigma_{\text{A}}, \sigma'_{\text{B}}\rangle \quad (24\text{b})$$

with normalization constants N_Φ and N_Ψ . All information about the shape of the photon wave-packet as well as the cavity detuning, i.e., the differences between the two cavities is encoded into the linear coefficients which are given by

$$f_{\sigma, j} = \int \frac{dk}{2\pi} r_j(\omega_k; \sigma_j) f(k) e^{-i(\omega_k t - k x_j)}. \quad (25)$$

Here $x_j = \ell_j + \ell_0$ denotes the total distance, that has been taken by the photon from I through arm j to the detectors: ℓ_j is the path length of arm j and ℓ_0 is the distance from II to the detectors. From the general expressions (24) the ideal case is easily recovered: if the photon frequency is emitted exactly at the sweet spot $\omega_k = \Omega$ and if both cavities are identical, the projected states are equal to the favored Bell states $|\Phi^{\text{m}}\rangle = |\Phi^-\rangle$ and $|\Psi^{\text{m}}\rangle = |\Psi^-\rangle$.

However, if these conditions for the ideal case cannot be fulfilled, the projected state deviates from a maximally entangled state. This deviation can be quantified in terms of the fidelities of the measured states and the designated Bell-state of the ideal case,

$$F[|\Phi^{\text{m}}\rangle, |\Phi^-\rangle] = \frac{1}{2|N_\Phi|} |(f_{\uparrow, \text{A}} + f_{\uparrow, \text{B}}) - (f_{\downarrow, \text{A}} + f_{\downarrow, \text{B}})|^2, \quad (26)$$

$$F[|\Psi^{\text{m}}\rangle, |\Psi^-\rangle] = \frac{1}{2|N_\Psi|} |(f_{\uparrow, \text{A}} - f_{\downarrow, \text{B}}) - (f_{\downarrow, \text{A}} - f_{\uparrow, \text{B}})|^2. \quad (27)$$

So far, all expressions have been given in a general fashion including the effect of a photon wave-packet as well as the effect of detuned cavities. In the following these effects shall be discussed separately.

Lorentzian wave packet

To quantify the influence of a Lorentzian-shaped wave packet, the coefficients in Eq. (25) have to be evaluated for a Lorentzian envelope function

$$f(k) = \frac{\sqrt{c\Gamma}}{i(\omega_k - \Omega) - \Gamma/2}. \quad (28)$$

Here it is assumed that the central frequency of the envelope function equals the sweet spot frequency $\Omega = \omega_c \pm (\chi^2 - \kappa^2/4)^{1/2}$ in order to induce a π -phase shift, see Eq. (5). Since both cavities are considered to be equal in this case, the linear coefficients are symmetric with respect to exchange of the cavities, $f_{\sigma, \text{A}} = f_{\sigma, \text{B}}$. Therefore, we will omit the index j in the following. Then, the coefficients take two independent values f_\uparrow and $f_\downarrow = \eta f_\uparrow$ where η is a complex factor. Moreover, for a Lorentzian wave-packet these coefficients f_\uparrow , f_\downarrow , and η can be evaluated explicitly. In the limit of large cavity damping as compared to the photon line width $\Gamma \ll \kappa$, the η -factor becomes time-independent and reads

$$\eta(\Gamma) = \prod_{\nu=1}^2 \frac{i[\omega_c + (-1)^\nu \chi - \Omega] - \Gamma/2 + (-1)^\nu \kappa/2}{i[\omega_c + (-1)^\nu \chi - \Omega] - \Gamma/2 + (-1)^{\nu-1} \kappa/2}. \quad (29)$$

Here the difference between the optical path lengths has been set to zero, i.e., $\theta = 0$. Together with Eq. (29) the fidelities evaluate to

$$F[|\Phi^{\text{m}}\rangle, |\Phi^-\rangle] = \frac{1 + |\eta(\Gamma)|^2 - 2|\eta(\Gamma)| \cos[\varphi(\Gamma)]}{3 + 3|\eta(\Gamma)|^2 + 2|\eta(\Gamma)| \cos[\varphi(\Gamma)]}, \quad (30)$$

$$F[|\Psi^{\text{m}}\rangle, |\Psi^-\rangle] = 1 \quad (31)$$

where $\varphi(\Gamma) = \arg[\eta(\Gamma)]$ denotes the frequency-averaged phase difference.

As explained in the main text, the relative phase difference of states with even parity becomes zero $\varphi_\uparrow - \varphi_\downarrow = 0$, if the cavities are identical. Furthermore, these states (with equal phase difference) interfere destructively at the second beamsplitter and therefore not transmitted into channel D (parity-selective interference). Only states with odd parity are transmitted into channel D and by registering the photon there, the wave function is projected onto the Bell state with odd parity irrespective of the photon line width.

Detuned cavities

Microwave resonators, which are not identically fabricated, generally differ in their resonance frequencies,

$\omega_{c,A} \neq \omega_{c,B}$, their qubit couplings $\chi_A \neq \chi_B$, and their cavity broadenings $\kappa_A \neq \kappa_B$. Consequently, for a photon, that is emitted at a single frequency, it is impossible to match the sweet spot frequency for both cavities simultaneously, see Eq. (5). Assuming that the photon is emitted at frequency Ω_A , the scattering-induced phase difference is exactly π as indicated by the corresponding η -factor for cavity A, $\eta_A = f_{\downarrow,A}/f_{\uparrow,A} = e^{i\pi}$. However, since the photon frequency does not coincide with Ω_B , the corresponding η -factor for cavity B is $\eta_B = f_{\downarrow,B}/f_{\uparrow,B} = e^{i\varphi_B}$ with $\varphi_B \neq \pi$. In addition, arising due to the detuning of the cavities, the complex factor $\eta_{AB} = f_{\uparrow,B}/f_{\uparrow,A} \neq 1$ can be defined in analogy to η_A and η_B . Since we neglect the influence of a finite line width of the photon here, all linear coefficients $f_{\sigma,j}$ and their corresponding η -factors are complex phase factors with modulus one.

One might expect that η_{AB} has an influence on the fidelity, but fortunately this phase shift can be compensated by appropriately adjusting the optical path lengths inside the MZI. By using (25) we find

$$\eta_{AB} = \frac{f_{\uparrow,B}}{f_{\uparrow,A}} = \frac{r_B(\Omega_A; \uparrow)}{r_A(\Omega_A; \uparrow)} e^{i\Omega_A(\ell_B - \ell_A)/c}. \quad (32)$$

Hence, by properly tuning the angle θ of the interferometer, $\eta_{AB} = 1$ can be achieved.

* ohm@physik.rwth-aachen.de

- [1] R. Horodecki, P. Horodecki, M. Horodecki, and K. Horodecki, *Rev. Mod. Phys.* **81**, 865 (2009).
- [2] A. Einstein, B. Podolsky, and N. Rosen, *Phys. Rev.* **47**, 777 (1935).
- [3] C. H. Bennett, G. Brassard, C. Crépeau, R. Jozsa, A. Peres, and W. K. Wootters, *Phys. Rev. Lett.* **70**, 1895 (1993).
- [4] A. K. Ekert, *Phys. Rev. Lett.* **67**, 661 (1991).
- [5] B. Yurke and D. Stoler, *Phys. Rev. Lett.* **68**, 1251 (1992).
B. Yurke and D. Stoler, *Phys. Rev. A* **46**, 2229 (1992).
- [6] M. Żukowski, A. Zeilinger, M. A. Horne, and A. K. Ekert, *Phys. Rev. Lett.* **71**, 4287 (1993).
- [7] H.-J. Briegel, W. Dür, J. I. Cirac, and P. Zoller, *Phys. Rev. Lett.* **81**, 5932 (1998).
- [8] C. Cabrillo, J. I. Cirac, P. García-Fernández, and P. Zoller, *Phys. Rev. A* **59**, 1025 (1999).
- [9] M. B. Plenio, S. F. Huelga, A. Beige, and P. L. Knight, *Phys. Rev. A* **59**, 2468 (1999).
- [10] C. W. Chou, H. de Riedmatten, D. Felinto, S. V. Polyakov, S. J. van Enk, and H. J. Kimble, *Nature* **438**, 828 (2005).
- [11] D. L. Moehring, P. Maunz, S. Olmschenk, K. C. Younge, D. N. Matsukevich, L. M. Duan, and C. Monroe, *Nature* **449**, 68 (2007).
- [12] J. Hofmann, M. Krug, N. Ortengel, L. Gérard, M. Weber, W. Rosenfeld, and H. Weinfurter, *Science* **337**, 72 (2012).
- [13] H. Bernien, B. Hensen, W. Pfaff, G. Koolstra, M. S. Blok, L. Robledo, T. H. Taminiau, M. Markham, D. J. Twitchen, L. Childress, and R. Hanson, *Nature* **497**, 86 (2013).
- [14] N. Roch, M. E. Schwartz, F. Motzoi, C. Macklin, R. Vijay, A. W. Eddins, A. N. Korotkov, K. B. Whaley, M. Sarovar, and I. Siddiqi, *Phys. Rev. Lett.* **112**, 170501 (2014).
- [15] Y. P. Huang and M. G. Moore, *Phys. Rev. A* **77**, 032349 (2008).
- [16] A. Wallraff, D. I. Schuster, A. Blais, L. Frunzio, R. S. Huang, J. Majer, S. Kumar, S. M. Girvin, and R. J. Schoelkopf, *Nature* **431**, 162 (2004).
- [17] D. Riste, M. Dukalski, C. A. Watson, G. de Lange, M. J. Tiggelman, Y. M. Blanter, K. W. Lehnert, R. N. Schouten, L. DiCarlo, *Nature* **502**, 350 (2013).
- [18] A. Roy, L. Jiang, A. D. Stone, and M. H. Devoret, *arXiv:1505.01178* (2015).
- [19] M. Silveri, E. Zaly-Geller, M. Hatridge, Z. Leghtas, M. H. Devoret, and S. M. Girvin, *arXiv:1507.00732* (2015).
- [20] C. L. Hutchison, J. M. Gambetta, A. Blais, and F. K. Wilhelm, *Canadian Journal of Physics* **87**, 225 (2009).
- [21] K. Lalumière, J. M. Gambetta, and A. Blais, *Phys. Rev. A* **81**, 040301 (2010).
- [22] F. Helmer and F. Marquardt, *Phys. Rev. A* **79**, 052328 (2009).
- [23] L. S. Bishop, L. Tornberg, D. Price, E. Ginossar, A. Nunnenkamp, A. A. Houck, J. M. Gambetta, J. Koch, G. Johansson, S. M. Girvin, and R. J. Schoelkopf, *New J. Phys.* **11**, 073040 (2009).
- [24] A. A. Houck, D. I. Schuster, J. M. Gambetta, J. A. Schreier, B. R. Johnson, J. M. Chow, L. Frunzio, J. Majer, M. H. Devoret, S. M. Girvin, and R. J. Schoelkopf, *Nature* **449**, 328 (2007).
- [25] C. Eichler, C. Lang, J. M. Fink, J. Govenius, S. Filipp, and A. Wallraff, *Phys. Rev. Lett.* **109**, 240501 (2012).
- [26] R. Ruskov and A. N. Korotkov, *Phys. Rev. B* **67**, 241305 (2003).
- [27] C. W. J. Beenakker, D. P. DiVincenzo, C. Emary, and M. Kindermann, *Phys. Rev. Lett.* **93**, 020501 (2004).
- [28] A. N. Jordan, C. W. J. Beenakker, and M. Büttiker, *Phys. Rev. B* **73**, 235331 (2006).
- [29] N. S. Williams and A. N. Jordan, *Phys. Rev. A* **78**, 062322 (2008).
- [30] G. Haack, H. Förster, and M. Büttiker, *Phys. Rev. B* **82**, 155303 (2010).
- [31] D. F. Walls and G. J. Milburn, *Quantum Optics* (Springer-Verlag, Berlin, 2008).
- [32] G. Romero, J. J. García-Ripoll, and E. Solano, *Phys. Rev. Lett.* **102**, 173602 (2009).
- [33] M. P. da Silva, D. Bozyigit, A. Wallraff, and A. Blais, *Phys. Rev. A* **82**, 043804 (2010).
- [34] D. Bozyigit, C. Lang, L. Steffen, J. M. Fink, C. Eichler, M. Baur, R. Bianchetti, P. J. Leek, S. Filipp, M. P. da Silva, A. Blais, and A. Wallraff, *Nature Phys.* **7**, 154 (2011).
- [35] M. A. Nielsen and I. L. Chuang, *Quantum Computation and Quantum Information* (Cambridge University Press, Cambridge, 2010).
- [36] In the case $2\chi = \kappa$, the first non-vanishing contributions of Eqs. (8) and (10) appear to forth order in Γ/κ and $\delta\omega/\kappa$.
- [37] C. W. Gardiner and M. J. Collett, *Phys. Rev. A* **31**, 3761 (1985).